ACS APPLIED MATERIALS & INTERFACES

www.acsami.org

Research Article

# Trojan Horse Thiocyanate: Induction and Control of High Proton Conductivity in CPO-27/MOF-74 Metal–Organic Frameworks by Metal Selection and Solvent-Free Mechanochemical Dosing

Magdalena Lupa, Paweł Kozyra, Gabriela Jajko, and Dariusz Matoga*

Cite This: *ACS Appl. Mater. Interfaces* 2021, 13, 29820–29826

Read Online

ACCESS | Metrics & More | Article Recommendations | Supporting Information

**ABSTRACT:** Proton-conducting metal–organic frameworks (MOFs) have been gaining attention for their role as solid-state electrolytes in various devices for energy conversion and storage. Here, we present a convenient strategy for inducing and tuning of superprotonic conductivity in MOFs with open metal sites via postsynthetic incorporation of charge carriers enabled by solvent-free mechanochemistry and anion coordination. This scalable approach is demonstrated using a series of **CPO-27/MOF-74** [$M_2$(dobdc); M = $Mg^{2+}$, $Zn^{2+}$, $Ni^{2+}$; dobdc = 2,5-dioxido-1,4-benzenedicarboxylate] materials loaded with various stoichiometric amounts of $NH_4SCN$. The modified materials are not achievable by conventional immersion in solutions. Periodic density functional theory (DFT) calculations, supported by infrared (IR) spectroscopy and powder X-ray diffraction, provide structures of the modified MOFs including positions of inserted ions inside the [001] channels. Despite the same type and concentration of proton carriers, the MOFs can be arranged in the increasing order of conductivity (Ni < Zn < Mg), which strongly correlates with amounts of water vapor adsorbed. We conclude that the proton conductivity of **CPO-27** materials can be controlled over a few orders of magnitude by metal selection and mechanochemical dosing of ammonium thiocyanate. The dosing of a solid is shown for the first time as a useful, simple, and ecological method for the control of material conductivity.

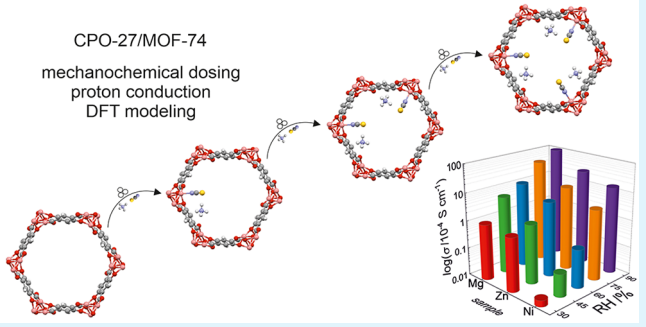


**KEYWORDS:** *synthesis, mechanochemistry, metal–organic frameworks, proton transport, adsorption*

## INTRODUCTION

Development of proton-conducting materials and gaining control of the conductivity are important both for fundamental understanding of charge transport phenomena as well as potential applications in sensors and polymer electrolyte membrane fuel cells (PEMFCs).[1,2] Within the last decade, metal–organic frameworks (MOFs) emerged as a class of compounds suitable for these purposes, due to their high performance and designability.[3−6] The literature contains several competing methods for inducing proton conductivity in MOFs which generally fall into two main categories. The first approach, known as the *de novo* synthesis, requires nonpolymeric building blocks and leads to the installation of Brønsted acidic centers either as linker pendant groups, guests, or terminal ligands. This approach, however, has serious limitations regarding inducing and control of conductivity in resultant frameworks. Direct introducing of linkers with acidic substituents is often hindered by their strong affinity toward metallic centers, which may consequently lead to undesired coordination and nonconducting products.[7] Similarly, direct *de novo* introducing of charged guests or terminal ligands as proton carriers is often serendipitous as highly dependent on uncontrolled pH changes during framework assembly. A promising and effective alternative is offered by the second main approach toward proton-conducting MOFs that relies on postsynthetic modifications (PSMs) of preassembled frameworks.[8] Within this approach, several proton-conducting MOFs were obtained via impregnation of parent MOFs with inorganic acids[9] or protic organic molecules.[10] Other distinct examples include organic linker modifications such as oxidation of thiol groups[11] or ring-opening reactions with sultones.[12] Finally, the combined *de novo* and PSM approaches can lead to a significant rise in conductivity, like in the MIL-101 platform in which pendant $SO_3H$ groups were first installed (MIL-101-$SO_3H$)[13] and then nonvolatile strong acid was introduced to form $H_2SO_4$@MIL-101-$SO_3H$ of excellent superprotonic conductivity.[14] It is noteworthy, however, that all the abovementioned synthetic approaches toward proton-

Received: April 6, 2021
Accepted: June 7, 2021
Published: June 17, 2021

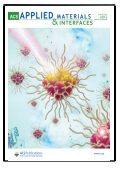

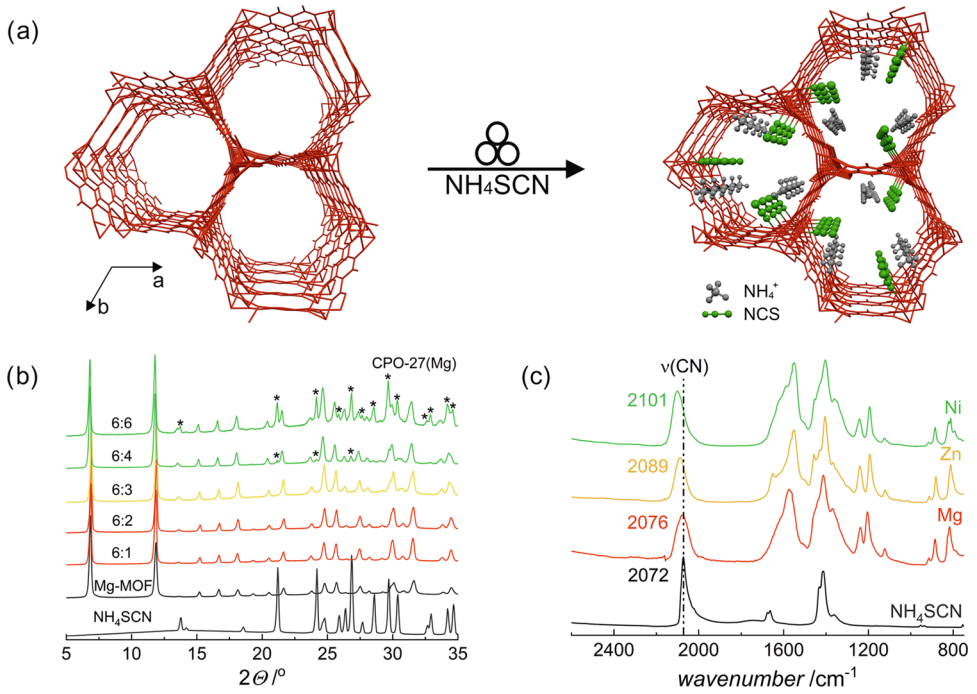


**Figure 1.** Solid-state reaction of **CPO-27** with $NH_4SCN$: (a) general scheme for the mechanochemical synthesis of **CPO-27-NCS**; (b) PXRD patterns of mixtures after grinding **CPO-27(Mg)** with various amounts of $NH_4SCN$; 6:1, 6:2, 6:3, 6:4, and 6:6 (given as **CPO-27(Mg)** to $NH_4SCN$ stoichiometric ratio). Characteristic reflections of $NH_4SCN$ are labeled with "*"; and (c) FT-IR spectra of **CPO-27(Mg)-NCS**, **CPO-27(Zn)-NCS**, and **CPO-27(Ni)-NCS**. Numbers indicate wavenumbers (in $cm^{-1}$) of the characteristic CN stretches.

conducting MOFs usually involve complicated steps, require large amounts of solvents and energy, are difficult to upscale, and do not allow for control of proton conductivity.

As a remedy for typically complicated, costly, and non-ecological syntheses in solution, a facile solvent-free mechanochemical approach, which is established in organic,[15] organometallic[16] and main group chemistry,[17] and also enables large-scale synthesis,[18−23] has increasingly become an alternative consideration for the preparation of various functional materials including porous MOFs.[24] Even though mechanochemistry is not widely used to induce proton conductivity in MOFs, there are a few distinct reports in the literature. Among initial mechanochemical syntheses of proton-conducting MOFs were those described by Horike, Kitagawa, and others who carried out grinding of zinc oxide with azoles and orthophosphates, followed by the demonstration of intrinsic proton conduction of the resulting frameworks.[25,26] Using the same mechanochemical approach for analogous systems, these researchers also reported the formation of a glassy state of a MOF that exhibited enhanced proton conductivity by 2 orders of magnitude as compared to its crystalline form.[27] In 2015, we carried out a unique postsynthetic modification of $\{[Mn_2(ina)_4(H_2O)_2]\cdot 2EtOH\}_n$[28] (JUK-1) by grinding it with an ionic compound that yielded a proton-conducting $\{(NH_4)_2[Mn(ina)_2(NCS)_2]\}_n\cdot xH_2O$ (JUK-2).[29] This fast and stoichiometric solid-state reaction led to a significant structural reconfiguration of the parent framework involving unzipping of crystalline JUK-1 bilayers to JUK-2 monolayers.[30]

While mechanochemical syntheses of MOFs are gaining impetus, the use of mechanochemical methods for tuning of either ionic or electronic conductivity of these materials has not been reported so far. In the literature, a remarkable tuning of electrical conductivity in MOFs was previously demonstrated for HKUST-1 infiltrated by a redox-active 7,7,8,8-tetracyanoquinodimethane (TCNQ) molecule.[31] However, the tuning was achieved by controlling of exposure (immersion) time of the MOF in a saturated $TCNQ/CH_2Cl_2$ solution. It is worth noting that tunability of conductivity is not only necessary to obtain the value as high as possible (e.g., for PEMFCs), it is also important to tailor materials conductivity for some specific applications, e.g., in devices for energy conversion and information transfer, such as sensors, capacitors, memristors, transistors, and batteries.

In this work, we report a convenient and facile strategy for realizing postsynthetic tunable proton conductivity in MOFs by scalable solvent-free mechanochemistry. We demonstrate that grinding rigid **CPO-27/MOF-74(Mg, Zn, Ni)** materials with $NH_4SCN$ leads to a series of functionalized charged frameworks whose channels, filled with counterbalancing ions, become suitable for proton transport. Contrary to our precedent case study involving JUK-2,[29] the mechanochemical reactions carried out in this work lead to virtually intact networks, and the highest proton conductivities of the modified frameworks 10-fold exceed that of JUK-2. The structures for the modified MOFs are provided by density functional theory (DFT) calculations and are corroborated by vibrational spectroscopy and powder X-ray diffraction (PXRD). The conducting properties of all materials are compared and discussed. Mechanochemical stoichiometric dosing of an ionic compound is shown for the first time as a useful, simple, and scalable method for the control of material conductivity.

## RESULTS AND DISCUSSION

The family of **CPO-27(M)** MOFs (M = Mn, Mg, Fe, Co, Ni, Cu, and Zn) is known for relatively stable structures containing one-dimensional channels with open metal sites.[32] *N,N′*-dimethylformamide (DMF) molecules coordinated to metallic


https://doi.org/10.1021/acsami.1c06346
ACS Appl. Mater. Interfaces 2021, 13, 29820−29826

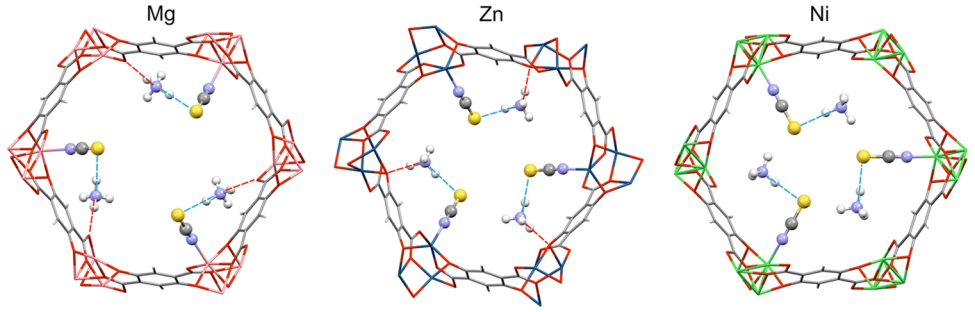


**Figure 2.** Structures of **CPO-27-NCS** optimized by periodic DFT+D methods, view along the [001] channels (Mg, Zn—full optimization; Ni—framework atoms frozen). Hydrogen bonds involving $NH_4^+$ ions are indicated by red (N−H···O) and cyan (N−H···S) dotted lines between donor and acceptor atoms. Color codes: C—gray, H—light gray, N—blue, O—red, and S—yellow.

centers in the as-synthesized materials can be replaced with methanol or water and removed by heating under vacuum.[33] The channels can be decorated by functional molecules for the application of interest. Recent literature examples show that the coordinative insertion of *N,N′*-dimethylethylenediamine enhances $CO_2$ adsorption,[34] whereas the insertion of urea enables highly stable superprotonic conductivity.[35] In this work, we have carried out new scalable modifications of **CPO-27** series and prepared three compounds with coordinated thiocyanates: $(NH_4)_3[Mg_6(dobdc)_3(NCS)_3(H_2O)_3]\cdot xH_2O$ (**CPO-27(Mg)-NCS**), $(NH_4)_3[Zn_6(dobdc)_3(NCS)_3(DMF)(H_2O)_2]\cdot xH_2O$ (**CPO-27(Zn)-NCS**), and $(NH_4)_3[Ni_6(dobdc)_3(NCS)_3(H_2O)_3]\cdot xH_2O$ denoted as **CPO-27(Ni)-NCS** (Figures 1 and S1). Regardless of the metal used, after grinding of **CPO-27** and $NH_4SCN$ with the addition of a small amount of EtOH, rigid frameworks remain virtually intact (as confirmed by PXRD patterns), whereas the evidence for the coordination of thiocyanate is provided by the infrared (IR) shift of the strong $\nu$(CN) band from 2072 (for the initial $NH_4SCN$) to 2076, 2089, and 2101 $cm^{-1}$ for **CPO-27(Mg)-NCS**, **CPO-27(Zn)-NCS**, and **CPO-27(Ni)-NCS**, respectively (Figures 1, S1, and S2). The mechanochemical reactions are fast, stoichiometric, and occur with retainment of crystallinity. The maximal stoichiometry of these reactions was determined to be 6:3 (metal/thiocyanate ratio) for the three MOFs, as evidenced collectively by powder X-ray diffraction (XRD) and IR spectroscopy (Figures 1, S2, and S3). The maximally loaded **CPO-27-NCS** materials show practically no uptake of nitrogen and argon (Figures S4 and S5), as compared to high uptakes reported in the literature for the **CPO-27** materials, synthesized both in water and by solvent-free grinding, which indicates filling the pores of **CPO-27** by ammonium thiocyanate.[36,37] The reactions carried out at higher stoichiometric ratios (6:4 and 6:6) gave mixtures of uncoordinated thiocyanate and **CPO-27-NCS** (observable by the appearance of extra X-ray reflections of $NH_4SCN$ and/or extra ν(CN) IR bands), whereas the use of lower stoichiometric ratios (6:2 and 6:1) led to partial filling of channels with coordinated $NCS^-$ and extra-framework $NH_4^+$ ions. The unique reactivity of the **CPO-27** materials opens possibilities for tuning of their properties by mechanochemical dosing of thiocyanates with other counterions.

To verify the possibilities of both formation of **CPO-27-NCS** and tuning of their proton conductivities in solution, **CPO-27(Mg, Zn, Ni)** MOFs were immersed in alcohol solutions (methanol or ethanol) containing $NH_4SCN$ at various $SCN^-$ to MOF ratios (see the Supporting Information for details, Figures S6 and S7). Under no conditions we have tried the formation of **CPO-27-NCS** was observed, which proves the necessity of mechanical grinding in yielding **CPO-27-NCS**. Furthermore, given the recent demonstration of efficient gram-scale mechanosynthesis of **CPO-27(Zn)**,[36] it is noteworthy that **CPO-27(Zn)-NCS** can be entirely prepared from simple nonpolymeric precursors in a two-step mechanosynthesis. The second mechanochemical step can be reversed by immersing the modified materials in alcohols for several days at elevated temperature, which leads to recovery of initial **CPO-27** materials upon removal of coordinated thiocyanates (Figure S8).

Insights into the structures of the modified MOFs were provided by periodic DFT+D calculations (see the Supporting Information for details). Our experimental XRD data did not allow us to unambiguously locate the positions of $NH_4^+$ and $SCN^-$ ions in the structure using Rietveld refinement (see the Supporting Information for details). We have taken under consideration the structures of **CPO-27(Mg, Zn, Ni)** with $SCN^-$ anions inserted inside the [001] channels at the metal-to-thiocyanate ratio of 6:3. DFT optimizations were carried out for two possible linkage isomers with either S- or N-bound thiocyanate. In the simplified model, the **CPO-27** framework atoms were frozen. The calculated total energies for **CPO-27-NCS** and **CPO-27-SCN** optimized structures proved similar (for a given metal) and did not allow for the unambiguous discrimination between the two binding modes. Thus, full structural optimizations, which allowed a vibrational analysis, were performed for **CPO-27(Mg)-NCS**, **CPO-27(Mg)-SCN**, **CPO-27(Zn)-NCS**, and **CPO-27(Zn)-SCN**. Since the energies for the two linkage isomers within this approach were similar again, we have taken CN stretch wavenumbers as an indicator of the coordination mode of thiocyanate. The calculations clearly demonstrate that these wavenumbers are higher for M-NCS structures, with shorter CN bonds. To compare experimental IR wavenumbers for the modified **CPO-27** MOFs with those calculated for the two binding variants, we have scaled our method by performing vibrational analysis for the selected monomeric thiocyanate complexes containing either of the three Mg, Zn or Ni metals. The Cambridge Structural Database (CSD) database search gave a few structurally characterized compounds including two complexes of $[Zn(NCS)_4]^{2-}$ (CSD codes: MENBEM, MUDPIM, NESMOP)[38−40] and $[Ni(NCS)_6]^{4-}$ (CSD codes: FILVAA, YIGGIH01)[41,42] whose averaged experimental CN wavenumbers were 2085 and 2095 $cm^{-1}$, respectively. Their comparison with the values calculated by our method (2113 and 2119 $cm^{-1}$, respectively) allowed us to estimate the scaling factor for the method as 0.988 (experimental/calculated),


https://doi.org/10.1021/acsami.1c06346
ACS Appl. Mater. Interfaces 2021, 13, 29820−29826

which was applied for the calculated raw wavenumbers in the modified **CPO-27**, and the scaled values were compared with the experimental wavenumbers (see Table S1). The scaled CN stretches for Mg- and Zn-based structures with N-bound thiocyanates match the experimental values very well. Similarly, the CN stretches estimated for the modified **CPO-27(Ni)** indicate that the nickel-based structure contains the N-bound thiocyanate. All three **CPO-27-NCS** structures, optimized by DFT methods, are presented in Figure 2.

The optimized structures show significant differences in the location of ammonium ions inside the [001] channels (Figure 2). In all of the modified frameworks, ammonium ions are hydrogen-bonded with sulfur atoms of N-coordinated thiocyanates. These hydrogen bonds increase in strength as the average donor−acceptor distances (N···S) decrease in the order: Ni (3.35 Å) < Zn (3.27 Å) < Mg (3.14 Å), and the corresponding average N−H bonds are elongated: 1.066 Å (Ni) < 1.068 Å (Zn) < 1.089 Å (Mg) accordingly (Table 1).

**Table 1. Hydrogen Bond Distances (Averaged, in Å) Involving $NH_4^+$ Ions Inside CPO-27-NCS**

| | | Mg | Zn | Ni |
|---|---|---|---|---|
| N−H···S | *d*(NS) | 3.14 | 3.27 | 3.35 |
| | *d*(NH) | 1.089 | 1.068 | 1.066 |
| N−H···O | *d*(NO) | 2.92 | 2.74 | |
| | *d*(NH) | 1.046 | 1.071 | |

Apart from interactions with sulfur atoms, ammonium ions in **CPO-27(Zn, Mg)-NCS** are additionally stabilized by strong hydrogen bonds with intraframework oxygen atoms, which are also accountable for N−H bond elongations. The longer N−H bonds are, the higher proton mobility is inside MOF channels and, consequently, material conductivity.

In the literature, the recently reported studies for a single crystal of **CPO-27(Co)** showed that proton conduction of the material was anisotropic and occurred predominantly through one-dimensional channels (intrachannel proton conductivity at 25−30 °C was ~$10^{-4}$ S $cm^{-1}$ in contrast to perpendicular directions with $\sigma \sim 10^{-6}$ S $cm^{-1}$).[43,44] It is justified to assume that the same intrachannel pathways are mainly responsible for proton conduction of other isoreticular **CPO-27** MOFs and their modifications with retained framework structures, such as the **CPO-27-NCS** materials in this work. During solvent-free grinding of **CPO-27(Co)** and ammonium thiocyanate, we have observed partial decomposition of **CPO-27(Co)** and the formation of $[Co(NCS)_4]^{2-}$ ions (the Vogel reaction),[45,46] identifiable by the appearance of blue color (see Figure S11). However, the solvent-free reactions of **CPO-27(Mg, Zn, Ni)** MOFs with $NH_4SCN$ yielded **CPO-27-NCS** with ammonium proton carriers inside their unidirectional channels and induced high proton conductivity in the modified materials. This functionalization was enabled using thiocyanates as Trojan horse anions "carrying" counterbalancing protic cations. For proton conduction studies of the modified MOFs, alternating current (AC) impedance measurements were carried out using powdered samples pressed between metallic electrodes in a poly(tetrafluoroethylene) (PTFE) tube under different RH values from 30 to 90%, and variable temperatures from 25 to 60 °C (Figures 3 and S12−S16). The highest proton conductivities in the series, reaching $10^{-2}$ S $cm^{-1}$ at high relative humidity (60 °C, 90% RH) and $10^{-4}$ S $cm^{-1}$ already at 30% RH, were observed for **CPO-27(Mg)-NCS**. Despite the same type and concentration of proton carriers, the other two materials, **CPO-27(Zn, Ni)-NCS** showed lower values (Figure 3 and Table S2) and the whole series can be arranged in the decreasing order of conductivity: Mg > Zn > Ni. The series correlates well with the decreasing hydrophilicity of the MOFs, confirmed by their water vapor uptake isotherms (Figure 4). The isotherms also show the stability of the materials during adsorption−desorption cycling (Figure S24) as well as significant differences between the three MOFs including highest uptakes and conductivities for **CPO-27(Mg)-NCS** and the lowest for **CPO-27(Ni)-NCS**. The nanoconfinement of $NH_4SCN$ within the [001] channels of **CPO-27** materials has a double effect on conductivity: (i) it induces high proton conductivity of **CPO-27** through introducing extra-framework proton carriers and (ii) it modulates the ability of **CPO-27** to adsorb water molecules that are essential elements of conduction pathways. The latter strongly depends on the selection of a metal center in the **CPO-27** material. By metal selection (Mg, Zn, or Ni) and RH adjustment, proton conductivity of **CPO-27-NCS** can be controlled over 3 orders of magnitude (Figure 3c). It is likely that further finetuning might be achieved using various mixed-metal **CPO-27** frameworks, whose mechanochemical syntheses have been recently reported in the literature.[47] Interestingly, apart from appropriate metal selection, proton conductivities of **CPO-27-NCS** can be additionally controlled by mechanochemical stoichiometric dosing of thiocyanate ions within

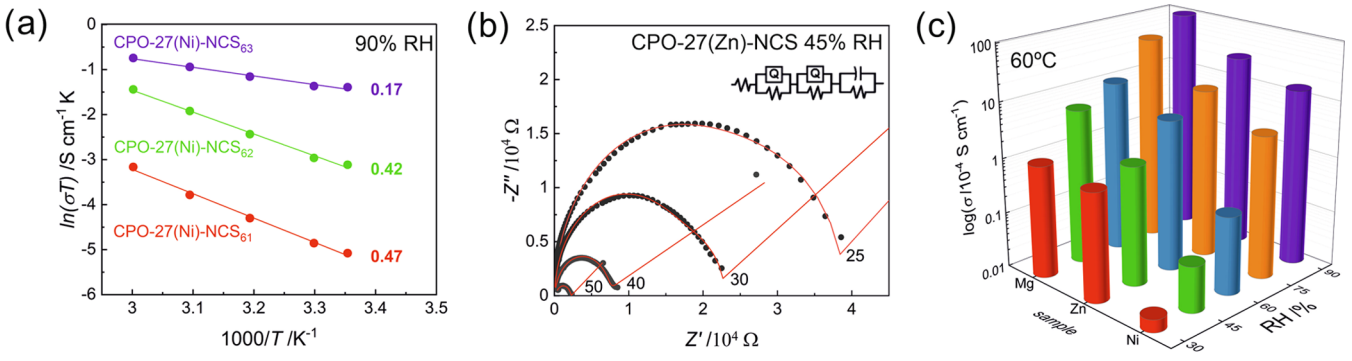


**Figure 3.** Proton conduction for **CPO-27-NCS**: (a) Arrhenius plots with activation energies indicated as numbers (in eV) after mechanochemical dosing of $NH_4SCN$ in **CPO-27(Ni)-NCS** (with 6:1, 6:2, and 6:3 metal/thiocyanate ratios); samples conditioned at 90% RH. (b) Temperature-dependent AC impedance plots for **CPO-27(Zn)-NCS** at 45% RH (maximal $NH_4SCN$ loading, numbers indicate temperatures in °C) with equivalent circuit used for fitting plots. (c) Proton conductivities at 60 °C and different RH values, all MOFs with maximal $NH_4SCN$ loading.



https://doi.org/10.1021/acsami.1c06346
ACS Appl. Mater. Interfaces 2021, 13, 29820−29826

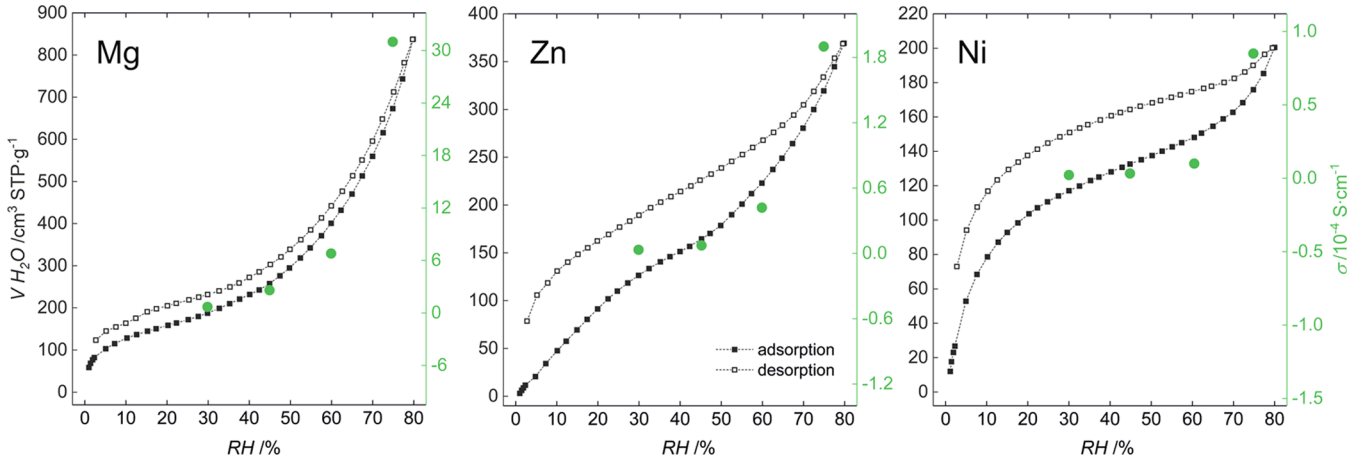


**Figure 4.** Proton conductivity versus water vapor adsorption−desorption isotherms for **CPO-27-NCS** (with maximal $NH_4SCN$ loading) at 25 °C.

the 6:1−6:3 metal-to-thiocyanate ratio range. Unattainable by immersion in solution, tunable proton conductivity over 1 order of magnitude was achieved for all **CPO-27-NCS** at 90% RH and 60 °C (Tables S3−S5 and Figures S19−S21). At lower temperatures, the tuning range depends on a metal center and is either slightly narrower or wider, with up to 2- (Zn), 6- (Mg), and 40-fold (Ni) increases of conductivity upon increase of the dose of $NH_4SCN$ from 6:1 to 6:3. The conductivities achieved for the largest 6:3 doses are among the highest reported for similar materials and significantly higher as compared to initial **CPO-27** MOFs (Table S6).

The linear regression of Arrhenius plots of the temperature-dependent proton conductivities of **CPO-27-NCS** provided activation energies ($E_a$) for proton transport inside their microporous channels at various RH values (Figures 3, S17, and S22). For two materials in the series, that is **CPO-27(Mg, Ni)-NCS**, the activation energies did not exceed 0.4 eV in the whole RH range, which shows that proton conduction occurs by a Grotthuss-type hopping mechanism, involving water molecules and ammonium cations. By contrast, proton conduction of **CPO-27(Zn)-NCS** is characterized by the increased $E_a$ values between 0.46 and 0.86 eV, which indicates the different mechanism of proton transport involving translational movements of $NH_4^+$ and $H_3O^+$ ions as well as their deprotonated counterparts (vehicle mechanism). In general, $NH_4^+$ conductors are promising materials for electrochemical devices such as fuel cells utilizing ammonia or ammonium salts.[48,49] The different mechanism for **CPO-27(Zn)-NCS** is likely associated with partial coordination of zinc metal centers with DMF molecules, whose presence disrupts the hydrogen bond network inside channels for proton hopping.

## CONCLUSIONS

We have reported a convenient strategy for realizing tunable proton conductivity in metal−organic frameworks in which micropores are loaded with protic guest cations by solvent-free mechanochemistry. This scalable and facile approach is demonstrated using a series of **CPO-27/MOF-74** materials loaded with ammonium thiocyanate. Tunable proton conductivities over 4 orders of magnitude are achieved in the whole series, with values as high as $10^{-2}$ S $cm^{-1}$. The strategy could be extended with other salts composed of protic ions and those capable of complexation. The targeted MOFs for such postsynthetic modifications should preferably contain under-coordinated open metal sites. The modified proton-conducting MOFs of good stability and high performance may have applications in devices such as fuel and solar cells as well as other devices for energy conversion and information transfer.

## ASSOCIATED CONTENT

### Supporting Information

The Supporting Information is available free of charge at https://pubs.acs.org/doi/10.1021/acsami.1c06346.

DFT optimized structure for **CPO-27(Mg)-NCS** (CIF)
DFT optimized structure for **CPO-27(Zn)-NCS** (CIF)
DFT optimized structure for **CPO-27(Ni)-NCS** (CIF)
Details of synthetic procedures, sample handling, physical measurements, and computational studies; additional IR, PXRD, EIS, and adsorption data (PDF)

## AUTHOR INFORMATION

### Corresponding Author

**Dariusz Matoga** − *Faculty of Chemistry, Jagiellonian University, 30-387 Kraków, Poland;* orcid.org/0000-0002-0064-5541; Email: dariusz.matoga@uj.edu.pl

### Authors

**Magdalena Lupa** − *Faculty of Chemistry, Jagiellonian University, 30-387 Kraków, Poland;* orcid.org/0000-0001-5818-7275

**Paweł Kozyra** − *Faculty of Chemistry, Jagiellonian University, 30-387 Kraków, Poland;* orcid.org/0000-0002-7168-5022

**Gabriela Jajko** − *Faculty of Chemistry, Jagiellonian University, 30-387 Kraków, Poland;* orcid.org/0000-0001-8286-917X

Complete contact information is available at: https://pubs.acs.org/10.1021/acsami.1c06346

### Author Contributions

M.L.: investigation, formal analysis, visualization, and writing—original draft preparation. P.K.: investigation (DFT calculations). G.J.: investigation (sorption measurements). D.M.: conceptualization, formal analysis, writing—original draft preparation, writing—review and editing, supervision, project administration, and funding acquisition.

### Notes

The authors declare no competing financial interest.

## ■ ACKNOWLEDGMENTS

The National Science Centre (NCN, Poland) is gratefully acknowledged for the financial support (Grant no. 2015/17/B/ST5/01190). The authors thank Prof. W. Makowski for the access to a volumetric gas adsorption analyzer.

## ■ REFERENCES

(1) Haile, S. M.; Boysen, D. A.; Chisholm, C. R. I.; Merle, R. B. Solid Acids as Fuel Cell Electrolytes. *Nature* **2001**, *410*, 910−913.
(2) Kreuer, K.-D. Proton Conductivity: Materials and Applications. *Chem. Mater.* **1996**, *8*, 610−641.
(3) Furukawa, H.; Cordova, K. E.; O'Keeffe, M.; Yaghi, O. M. The Chemistry and Applications of Metal-Organic Frameworks. *Science* **2013**, *341*, No. 1230444.
(4) Lim, D.-W.; Kitagawa, H. Proton Transport in Metal−Organic Frameworks. *Chem. Rev.* **2020**, *120*, 8416−8467.
(5) Ramaswamy, P.; Wong, N. E.; Shimizu, G. K. H. MOFs as Proton Conductors − Challenges and Opportunities. *Chem. Soc. Rev.* **2014**, *43*, 5913−5932.
(6) Xie, X.-X.; Yang, Y.-C.; Dou, B.-H.; Li, Z.-F.; Li, G. Proton Conductive Carboxylate-Based Metal−Organic Frameworks. *Coord. Chem. Rev.* **2020**, *403*, No. 213100.
(7) Szufla, M.; Roztocki, K.; Krawczuk, A.; Matoga, D. One-Step Introduction of Terminal Sulfonic Groups into a Proton-Conducting Metal−Organic Framework by Concerted Deprotonation−Metalation−Hydrolysis Reaction. *Dalton Trans.* **2020**, *49*, 9953−9956.
(8) Kang, D. W.; Kang, M.; Hong, C. S. Post-Synthetic Modification of Porous Materials: Superprotonic Conductivities and Membrane Applications in Fuel Cells. *J. Mater. Chem. A* **2020**, *8*, 7474−7494.
(9) Ponomareva, V. G.; Kovalenko, K. A.; Chupakhin, A. P.; Dybtsev, D. N.; Shutova, E. S.; Fedin, V. P. Imparting High Proton Conductivity to a Metal−Organic Framework Material by Controlled Acid Impregnation. *J. Am. Chem. Soc.* **2012**, *134*, 15640−15643.
(10) Zhang, F.-M.; Dong, L.-Z.; Qin, J.-S.; Guan, W.; Liu, J.; Li, S.-L.; Lu, M.; Lan, Y.-Q.; Su, Z.-M.; Zhou, H.-C. Effect of Imidazole Arrangements on Proton-Conductivity in Metal−Organic Frameworks. *J. Am. Chem. Soc.* **2017**, *139*, 6183−6189.
(11) Phang, W. J.; Jo, H.; Lee, W. R.; Song, J. H.; Yoo, K.; Kim, B.; Hong, C. S. Superprotonic Conductivity of a UiO-66 Framework Functionalized with Sulfonic Acid Groups by Facile Postsynthetic Oxidation. *Angew. Chem., Int. Ed.* **2015**, *54*, 5142−5146.
(12) Mukhopadhyay, S.; Debgupta, J.; Singh, C.; Sarkar, R.; Basu, O.; Das, S. K. Designing UiO-66-Based Superprotonic Conductor with the Highest Metal−Organic Framework Based Proton Conductivity. *ACS Appl. Mater. Interfaces* **2019**, *11*, 13423−13432.
(13) Zhou, Y.-X.; Chen, Y.-Z.; Hu, Y.; Huang, G.; Yu, S.-H.; Jiang, H.-L. MIL-101-$SO_3$H: A Highly Efficient Brønsted Acid Catalyst for Heterogeneous Alcoholysis of Epoxides under Ambient Conditions. *Chem. − Eur. J.* **2014**, *20*, 14976−14980.
(14) Li, X.-M.; Dong, L.-Z.; Li, S.-L.; Xu, G.; Liu, J.; Zhang, F.-M.; Lu, L.-S.; Lan, Y.-Q. Synergistic Conductivity Effect in a Proton Sources-Coupled Metal−Organic Framework. *ACS Energy Lett.* **2017**, *2*, 2313−2318.
(15) Hernández, J. G.; Bolm, C. Altering Product Selectivity by Mechanochemistry. *J. Org. Chem.* **2017**, *82*, 4007−4019.
(16) Rightmire, N. R.; Hanusa, T. P. Advances in Organometallic Synthesis with Mechanochemical Methods. *Dalton Trans.* **2016**, *45*, 2352−2362.
(17) Tan, D.; García, F. Main Group Mechanochemistry: From Curiosity to Established Protocols. *Chem. Soc. Rev.* **2019**, *48*, 2274−2292.
(18) Crawford, D.; Casaban, J.; Haydon, R.; Giri, N.; McNally, T.; James, S. L. Synthesis by Extrusion: Continuous, Large-Scale Preparation of MOFs Using Little or No Solvent. *Chem. Sci.* **2015**, *6*, 1645−1649.
(19) Singh, V. K.; Chamberlain-Clay, A.; Ong, H. C.; León, F.; Hum, G.; Par, M. Y.; Daley-Dee, P.; García, F. Multigram Mechanochemical Synthesis of a Salophen Complex: A Comparative Analysis. *ACS Sustainable Chem. Eng.* **2021**, *9*, 1152−1160.
(20) Hong, Z.; Tan, D.; John, R. A.; Tay, Y. K. E.; Ho, Y. K. T.; Zhao, X.; Sum, T. C.; Mathews, N.; García, F.; Soo, H. S. Completely Solvent-Free Protocols to Access Phase-Pure, Metastable Metal Halide Perovskites and Functional Photodetectors from the Precursor Salts. *iScience* **2019**, *16*, 312−325.
(21) Colacino, E.; Isoni, V.; Crawford, D.; García, F. Upscaling Mechanochemistry: Challenges and Opportunities for Sustainable Industry. *Trends Chem.* **2021**, *3*, 335−339.
(22) Baláž, M.; Dobrozhan, O.; Tešinský, M.; Zhang, R.-Z.; Džunda, R.; Dutková, E.; Rajňák, M.; Chen, K.; Reece, M. J.; Baláž, P. Scalable and Environmentally Friendly Mechanochemical Synthesis of Nanocrystalline Rhodostannite ($Cu_2FeSn_3S_8$). *Powder Technol.* **2021**, *388*, 192−200.
(23) He, X.; Deng, Y.; Zhang, Y.; He, Q.; Xiao, D.; Peng, M.; Zhao, Y.; Zhang, H.; Luo, R.; Gan, T.; Ji, H.; Ma, D. Mechanochemical Kilogram-Scale Synthesis of Noble Metal Single-Atom Catalysts. *Cell Rep. Phys. Sci.* **2020**, *1*, No. 100004.
(24) Stolar, T.; Užarević, K. Mechanochemistry: An Efficient and Versatile Toolbox for Synthesis, Transformation, and Functionalization of Porous Metal−Organic Frameworks. *CrystEngComm* **2020**, *22*, 4511−4525.
(25) Umeyama, D.; Horike, S.; Inukai, M.; Itakura, T.; Kitagawa, S. Inherent Proton Conduction in a 2D Coordination Framework. *J. Am. Chem. Soc.* **2012**, *134*, 12780−12785.
(26) Horike, S.; Umeyama, D.; Inukai, M.; Itakura, T.; Kitagawa, S. Coordination-Network-Based Ionic Plastic Crystal for Anhydrous Proton Conductivity. *J. Am. Chem. Soc.* **2012**, *134*, 7612−7615.
(27) Chen, W.; Horike, S.; Umeyama, D.; Ogiwara, N.; Itakura, T.; Tassel, C.; Goto, Y.; Kageyama, H.; Kitagawa, S. Glass Formation of a Coordination Polymer Crystal for Enhanced Proton Conductivity and Material Flexibility. *Angew. Chem., Int. Ed.* **2016**, *55*, 5195−5200.
(28) Matoga, D.; Gil, B.; Nitek, W.; Todd, A. D.; Bielawski, C. W. Dynamic 2D Manganese(II) Isonicotinate Framework with Reversible Crystal-to-Amorphous Transformation and Selective Guest Adsorption. *CrystEngComm* **2014**, *16*, 4959−4962.
(29) Matoga, D.; Oszajca, M.; Molenda, M. Ground to Conduct: Mechanochemical Synthesis of a Metal−Organic Framework with High Proton Conductivity. *Chem. Commun.* **2015**, *51*, 7637−7640.
(30) Matoga, D.; Roztocki, K.; Wilke, M.; Emmerling, F.; Oszajca, M.; Fitta, M.; Bałanda, M. Crystalline Bilayers Unzipped and Rezipped: Solid-State Reaction Cycle of a Metal−Organic Framework with Triple Rearrangement of Intralayer Bonds. *CrystEngComm* **2017**, *19*, 2987−2995.
(31) Talin, A. A.; Centrone, A.; Ford, A. C.; Foster, M. E.; Stavila, V.; Haney, P.; Kinney, R. A.; Szalai, V.; Gabaly, F. E.; Yoon, H. P.; Léonard, F.; Allendorf, M. D. Tunable Electrical Conductivity in Metal-Organic Framework Thin-Film Devices. *Science* **2014**, *343*, 66−69.
(32) Rosi, N. L.; Kim, J.; Eddaoudi, M.; Chen, B.; O'Keeffe, M.; Yaghi, O. M. Rod Packings and Metal−Organic Frameworks Constructed from Rod-Shaped Secondary Building Units. *J. Am. Chem. Soc.* **2005**, *127*, 1504−1518.
(33) Dietzel, P. D. C.; Morita, Y.; Blom, R.; Fjellvåg, H. An In Situ High-Temperature Single-Crystal Investigation of a Dehydrated Metal-Organic Framework Compound and Field-Induced Magnetization of One-Dimensional Metal-Oxygen Chains. *Angew. Chem., Int. Ed.* **2005**, *44*, 6354−6358.
(34) McDonald, T. M.; Mason, J. A.; Kong, X.; Bloch, E. D.; Gygi, D.; Dani, A.; Crocellà, V.; Giordanino, F.; Odoh, S. O.; Drisdell, W. S.; Vlaisavljevich, B.; Dzubak, A. L.; Poloni, R.; Schnell, S. K.; Planas, N.; Lee, K.; Pascal, T.; Wan, L. F.; Prendergast, D.; Neaton, J. B.; Smit, B.; Kortright, J. B.; Gagliardi, L.; Bordiga, S.; Reimer, J. A.; Long, J. R. Cooperative Insertion of $CO_2$ in Diamine-Appended Metal-Organic Frameworks. *Nature* **2015**, *519*, 303−308.
(35) Sarango-Ramírez, M. K.; Lim, D.-W.; Kolokolov, D. I.; Khudozhitkov, A. E.; Stepanov, A. G.; Kitagawa, H. Superprotonic Conductivity in Metal−Organic Framework via Solvent-Free


https://doi.org/10.1021/acsami.1c06346
ACS Appl. Mater. Interfaces 2021, 13, 29820−29826

Coordinative Urea Insertion. *J. Am. Chem. Soc.* **2020**, *142*, 6861−6865.
(36) Julien, P. A.; Užarević, K.; Katsenis, A. D.; Kimber, S. A. J.; Wang, T.; Farha, O. K.; Zhang, Y.; Casaban, J.; Germann, L. S.; Etter, M.; Dinnebier, R. E.; James, S. L.; Halasz, I.; Friščić, T. In Situ Monitoring and Mechanism of the Mechanochemical Formation of a Microporous MOF-74 Framework. *J. Am. Chem. Soc.* **2016**, *138*, 2929−2932.
(37) Garzón-Tovar, L.; Carné-Sánchez, A.; Carbonell, C.; Imaz, I.; Maspoch, D. Optimised Room Temperature, Water-Based Synthesis of CPO-27-M Metal−Organic Frameworks with High Space-Time Yields. *J. Mater. Chem. A* **2015**, *3*, 20819−20826.
(38) Chen, H.-J.; Zhang, L.-Z.; Cai, Z.-G.; Yang, G.; Chen, X.-M. Organic−Inorganic Hybrid Materials Assembled through Weak Intermolecular Interactions. Synthesis, Structures and Non-Linear Optical Properties of $[4,4'\text{-BipyH}_2][M(NCS)_4]$ (M = $Mn^{2+}$, $Co^{2+}$ or $Zn^{2+}$; 4,4′-Bipy = 4,4′-Bipyridine). *J. Chem. Soc., Dalton Trans.* **2000**, 2463−2466.
(39) Ye, H.-Q.; Xie, J.-L.; Yu, J.-Y.; Liu, Q.-T.; Dai, S.-L.; Huang, W.-Q.; Zhou, J.-R.; Yang, L.-M.; Ni, C.-L. Syntheses, Crystal Structures, Luminescent Properties of Two New Molecular Solids with Tetra(Isothiocyanate)Zinc(II) and Substituted Benzyl Triphenylphosphonium Cations. *Synth. Met.* **2014**, *197*, 99−104.
(40) Briceño, A.; Hill, Y. Exploring the Use of Anionic Homoleptic Complexes as Templates in the Design of Photoreactive Multi-Component Supramolecular Assemblies. *CrystEngComm* **2012**, *14*, 6121.
(41) López Lago, E.; Seijas, J. A.; de Pedro, I.; Rodríguez Fernández, J.; Vázquez-Tato, M. P.; González, J. A.; Rilo, E.; Segade, L.; Cabeza, O.; Rodríguez Fernández, C. D.; Arosa, Y.; Algnamat, B. S.; Varela, L. M.; Troncoso, J.; de la Fuente, R. Structural and Physical Properties of a New Reversible and Continuous Thermochromic Ionic Liquid in a Wide Temperature Interval: $[BMIM]_4[Ni(NCS)_6]$. *New J. Chem.* **2018**, *42*, 15561−15571.
(42) Liu, J.; Zhang, S.; Zeng, Y.; Shu, X.; Du, Z.; He, C.; Zhang, W.; Chen, X. Molecular Dynamics, Phase Transition and Frequency-Tuned Dielectric Switch of an Ionic Co-Crystal. *Angew. Chem., Int. Ed.* **2018**, *57*, 8032−8036.
(43) Hwang, S.; Lee, E. J.; Song, D.; Jeong, N. C. High Proton Mobility with High Directionality in Isolated Channels of MOF-74. *ACS Appl. Mater. Interfaces* **2018**, *10*, 35354−35360.
(44) Javed, A.; Strauss, I.; Bunzen, H.; Caro, J.; Tiemann, M. Humidity-Mediated Anisotropic Proton Conductivity through the 1D Channels of Co-MOF-74. *Nanomaterials* **2020**, *10*, No. 1263.
(45) Vogel, H. W. Spectroskopische Notizen. *Ber. Dtsch. Chem. Ges.* **1879**, *12*, 2313−2316.
(46) Kolthoff, I. M. The Cobalt-Thiocyanate Reaction for the Detection of Cobalt and Thiocyanate. *Mikrochemie* **1930**, *8*, 176−181.
(47) Ayoub, G.; Karadeniz, B.; Howarth, A. J.; Farha, O. K.; Đilović, I.; Germann, L. S.; Dinnebier, R. E.; Užarević, K.; Friščić, T. Rational Synthesis of Mixed-Metal Microporous Metal−Organic Frameworks with Controlled Composition Using Mechanochemistry. *Chem. Mater.* **2019**, *31*, 5494−5501.
(48) Tao, Y.; Gibbons, W.; Hwang, Y.; Radermacher, R.; Wang, C. Electrochemical Ammonia Compression. *Chem. Commun.* **2017**, *53*, 5637−5640.
(49) Lan, R.; Tao, S. Ammonia Carbonate Fuel Cells Based on a Mixed $NH_4^+/H^+$ Ion Conducting Electrolyte. *ECS Electrochem. Lett.* **2013**, *2*, F37−F40.


https://doi.org/10.1021/acsami.1c06346
*ACS Appl. Mater. Interfaces* 2021, 13, 29820−29826